

D2C: Unlocking the Potential of Continuous Autoregressive Image Generation with Discrete Tokens

Panpan Wang^{1*} Liqiang Niu² Fandong Meng² Jinan Xu^{1†} Yufeng Chen¹ Jie Zhou²

¹Beijing Key Laboratory of Traffic Data Mining and Embodied Intelligence,
Beijing Jiaotong University, Beijing, China

²Pattern Recognition Center, WeChat AI, Tencent Inc, China

{panpwang, jaxu, chenyf}@bjtu.edu.cn
{poetniu, fandongmeng, withtomzhou}@tencent.com

Abstract

In the domain of image generation, latent-based generative models occupy a dominant status; however, these models rely heavily on image tokenizer. To meet modeling requirements, autoregressive models possessing the characteristics of scalability and flexibility embrace a discrete-valued tokenizer, but face the challenge of poor image generation quality. In contrast, diffusion models take advantage of the continuous-valued tokenizer to achieve better generation quality but are subject to low efficiency and complexity. The existing hybrid models are mainly to compensate for information loss and simplify the diffusion learning process. The potential of merging discrete-valued and continuous-valued tokens in the field of image generation has not yet been explored. In this paper, we propose **D2C**, a novel two-stage method to enhance model generation capacity. In the first stage, the discrete-valued tokens representing coarse-grained image features are sampled by employing a small discrete-valued generator. Then in the second stage, the continuous-valued tokens representing fine-grained image features are learned conditioned on the discrete token sequence. In addition, we design two kinds of fusion modules for seamless interaction. On the *ImageNet-256* benchmark, extensive experiment results validate that our model achieves superior performance compared with several continuous-valued and discrete-valued generative models on the class-conditional image generation tasks.

1. Introduction

During these years, discrete-valued generative models have made remarkable progress in the realm of image generation (Yu et al., 2022; Xie et al., 2024; Wu et al., 2024; Liu et al., 2024; Yu et al., 2024a). The discrete image tokenizer that converts encoded features of the image into discrete-valued tokens through vector quantization (Van Den Oord et al., 2017; Esser et al., 2021), is one of the particularly important components of autoregressive and masked image generation models. Afterwards, discrete image tokens are applied to various image understanding and generation tasks with the same paradigm as language tokens. Autoregressive model is one of the most popular solutions because of outstanding achievements in the field of linguistics and their own versatility and scalability. Autoregressive image generation models (Yu et al., 2021; Sun et al., 2024; Ma et al., 2024; Zhang et al., 2024b; Yu et al., 2024b; Luo et al., 2024; Yu et al., 2024a) following the next token prediction paradigm have shown great performance in text-to-image generation and class-to-image generation tasks. In addition to this, non-autoregressive approaches (Chang et al., 2022; Li et al., 2023b; Chang et al., 2023; Yu et al., 2024b; Chen et al., 2024) employ masked image models to predict multiple randomly masked tokens with bidirectional attention, which conforms to the bidirectional correlations essence of visual signals and accelerates the sampling speed in model inference process.

Concurrently, another predominant methods are continuous-valued generative models, which employ a continuous tokenizer to encode and decode the image without vector quantization (Kingma, 2013). Diffusion models (Song et al., 2020; Ho et al., 2020) are the most common methods in continuous-valued generative models, which recover latent space of image from random Gaussian noise through progressively denoising, such as LDM with the U-Net block (Rombach et al., 2022), DiT with the transformer block (Peebles & Xie, 2023). In addition, methods about merging

*Work was done when Panpan Wang was an intern at Pattern Recognition Center, WeChat AI, Tencent Inc, China.

†Jinan Xu is the corresponding author.

autoregressive model and diffusion model (Tschannen et al., 2023; Fan et al., 2024; Zhou et al., 2024; Zhao et al., 2024) are beginning to emerge. Although diffusion models achieve slightly better generation performance than discrete-valued generative models, the challenges of low computational efficiency and complicated structure are still unavoidable. Subsequently, MAR model (Li et al., 2024a) uses a small MLP network to iteratively denoise with autoregressive prior that achieves the trade-off between accuracy and speed in image generation.

However, it does not matter whether discrete-valued generative models or continuous-valued generative models, each still faces some challenges. Firstly, the discrete image tokenizer in discrete-valued generative models reveals poor reconstruction quality because quantizing continuous encoded image features to discrete-valued tokens results in information loss. Secondly, high computational complexity of continuous-valued generative models constrains training and inference speed while the complete model is applied to iteratively denoise on the entire image. Third, research into merging discrete-valued tokens with continuous-valued tokens has not yet been well developed.

To address these challenges, we introduce **D2C**, a simple and effective hybrid model that improves image generation quality through synergizing discrete-valued and continuous-valued tokens. Specifically, it is a two-stage autoregressive framework. In the first phase, we train a small discrete-valued autoregressive model to sample the discrete token sequence as the coarse-grained image features that can be decoded into a low-quality image. In the next phase, we optimize a hybrid autoregressive model to generate continuous-valued tokens as the fine-grained image features conditioned on class token and generated discrete-valued tokens. Then, the decoder of VAE model is employed to convert the generated continuous-valued tokens into a high-quality image as our model final output. For realizing seamless interaction between discrete-valued and continuous-valued tokens, we elaborately design two kinds of fusion modules, cross-attention module and q-former module. Currently, there are a couple of work, such as DisCo-Diff (Xu et al., 2024), HART (Tang et al., 2024) that are a little similar to our idea. But being different from them, discrete-valued and continuous-valued tokens are generated by different pre-trained image tokenizers in our method and the two can be decoded separately, each yielding an image. Besides, our model is a two-stage framework to achieve coarse-grained to fine-grained image generation.

To summarize, our contributions are:

- We propose a novel two-stage hybrid autoregressive framework, D2C, which enhances image generation quality with fusing the discrete-valued and continuous-valued tokens from the independently trained image

tokenizers.

- We design two kinds of fusion modules including cross-attention module and q-former module, to achieve seamless interaction between discrete-valued and continuous-valued tokens.
- To verify our model effectiveness and versatility, we conduct experiments on the *ImageNet-256* benchmark. Experimental results indicate that our model outperforms both previous continuous-valued and discrete-valued generative models on the class-to-image task. Our model is more faster than MAR on this task in inference.

2. Related Work

Continuous-valued image generation models mainly contain diffusion models and autoregressive models. Diffusion models (Ho et al., 2020; Rombach et al., 2022; Ho et al., 2022; Betker et al., 2023) are known as state-of-the-art methods due to high-quality visual generation, which generate the image through an iteratively denoising process on the entire image. At first, convolutional U-Net is the backbone architecture in latent diffusion models (Rombach et al., 2022; Podell et al., 2023). To improve scalability and efficiency, the architecture of transformer from Peebles & Xie (2023); Bao et al. (2023); Chen et al. (2023) is proposed to replace the U-Net. Currently, another research direction that synergizes the autoregressive model and the continuous-valued token is gradually rising. GIVT (Tschannen et al., 2023) employs continuous-valued tokens instead of discrete-valued tokens in an autoregressive sequence model. In addition, MAR (Li et al., 2024a) autoregressively generates continuous-valued tokens equipped with diffusion loss, while Fluid (Fan et al., 2024) scales up this idea to the text-to-image generation task. Besides, Transfusion (Zhou et al., 2024) and MonoFormer (Zhao et al., 2024) achieve autoregressive prediction and diffusion denoising on only one transformer architecture. And DART (Gu et al., 2024) supports autoregressively denoising within a non-Markovian diffusion framework to take full advantage of the generation trajectory. However, most of these models are limited by less efficient and complex diffusion structure.

Discrete-valued image generation models are based on autoregressive models and masked models. Pioneering research on this kind of models (Van Den Oord et al., 2016; Chen et al., 2020) focuses on the pixel level in image generation. Along with the emergence of VQVAE (Van Den Oord et al., 2017) and VQGAN (Esser et al., 2021), which quantize per patch of image to the nearest discrete token, discrete-valued models (Sun et al., 2024; Yu et al., 2024a) have become one of the mainstream methods in the domain of image generation. In order to improve the performance of

image tokenizer, various models have been proposed (Yu et al., 2021; Lee et al., 2022; Zheng et al., 2022; Huang et al., 2023b;a; Cao et al., 2023). However, there is still a serious problem, codebook collapse. Then regularization (Razavi et al., 2019; Zhang et al., 2023), codebook transfer (Zhang et al., 2024a), codebook optimization (Zheng & Vedaldi, 2023; Shi et al., 2024), lookup-free quantization (Yu et al., 2023) and codebook decomposition (Li et al., 2024b; Bai et al., 2024) are designed to address the codebook collapse issue and enhance image reconstruction quality. Moreover, Chang et al. (2022; 2023); Li et al. (2023b) utilize masked image models to improve sampling speed, while Weber et al. (2024) operates directly on bit tokens to make full use of the rich semantic information. There were also efforts to insert arbitrary token orders into autoregressive models to adapt inherently bidirectional correlations of visual signals (Yu et al., 2024a; Pang et al., 2024). However, information loss caused by vector quantization still remains a challenge in discrete-valued image generation models, which could weaken the model generative capacity.

In view of the fact that continuous-valued and discrete-valued models have demonstrated excellent performance separately, hybrid models fusing continuous-valued and discrete-valued tokens may be a new perspective in image generation models. DisCo-Diff (Xu et al., 2024) has attempted to augment the continuous diffusion model with complementary discrete-valued tokens, proving the feasibility and effectiveness of the hybrid model in image generation tasks. In addition, Hart (Tang et al., 2024) makes up for information loss of discrete-valued tokens with continuous-valued tokens. On this basis, we propose a two-stage hybrid autoregressive model to further improve the image generation quality following from coarse-grained to fine-grained rule.

3. Preliminaries

Autoregressive image generation models following the next token prediction paradigm generate a token sequence from left to right and one by one. Given a sequence of tokens $x = [x_1, x_2, \dots, x_n]$, where n is the length of the sequence. The autoregressive model is trained to model the probability distribution of next token depending on the past generated tokens:

$$p_\theta(x) = \prod_{i=1}^n p_\theta(x_i | x_1, x_2, \dots, x_{i-1}) \quad (1)$$

where θ denotes the model parameter. The goal of autoregressive model is to optimize the $p_\theta(x_i | x_1, x_2, \dots, x_{i-1})$ over all image token sequences that are generated by a discrete image tokenizer (Esser et al., 2021; Sun et al., 2024; Yu et al., 2024a). In general, the autoregressive model consists of a stack of transformer blocks with causal attention,

as shown in Eq.1. In order to satisfy the unidirectional characteristics of the autoregressive model, each image is converted into a 1-dimensional sequence in the raster scan order.

Masked image generation models following the masked tokens prediction paradigm generate a sequence in an out-of-order manner. Analogously, the image is firstly encoded and quantized by a discrete image tokenizer and then the image tokens are randomly selected as masked tokens (Chang et al., 2022; 2023; Weber et al., 2024). The masked models are optimized through maximizing the likelihood of the masked tokens conditioned on the unmasked tokens. The difference with the autoregressive models is that the masked models could predict multiple tokens at each step with bidirectional attention.

Diffusion loss with MLP is a novel loss function for each token that is a continuous-valued vector (Li et al., 2024a). Diffusion loss follows the same principle of denoising to model a probability distribution of x conditioned on both t and z following the diffusion models (Ho et al., 2020; Rombach et al., 2022; Peebles & Xie, 2023), denoted as $p(x|z, t)$:

$$\mathcal{L}(z, x) = \mathbb{E}_{\varepsilon, t} [\|\varepsilon - \varepsilon_\theta(x_t | t, z)\|^2] \quad (2)$$

Specifically, t is a time step of the noise schedule sampled from $\{1, \dots, T\}$. x_t is the noise-corrupted vector sampled from $x_t = \sqrt{\bar{\alpha}_t}x_0 + \sqrt{1 - \bar{\alpha}_t}\varepsilon$, a Markovian process, where $\bar{\alpha}_t$ is the hyper-parameter determined by the noise schedule, x_0 is original image and ε is the sampled Gaussian noise. A noise prediction network ε_θ is parameterized by θ , which is a small MLP network for iteratively denoising. In addition, z is a conditioning vector produced by a generative model. The denosing MLP is trained by minimizing the mean-squared error between the predicted noise and the ground truth Gaussian noise.

4. Method

Currently, enhancing image generative capacity with integration of discrete-valued and continuous-valued tokens is gaining prominence, and its effectiveness has been confirmed within the realm of diffusion models (Xu et al., 2024). The existing method of fusing continuous-valued and discrete-valued tokens in the autoregressive models is mainly to compensate for information loss caused by the vector quantization (Tang et al., 2024). But regrettably, the maximum attainable performance of this method is limited to the performance exhibited by the continuous-valued generation model. To break the ceiling and further improve the generative capability, we propose D2C, a two-stage autoregressive hybrid model following a progressive generation manner that generates the continuous-valued tokens condition on discrete-valued tokens. The key point is how to

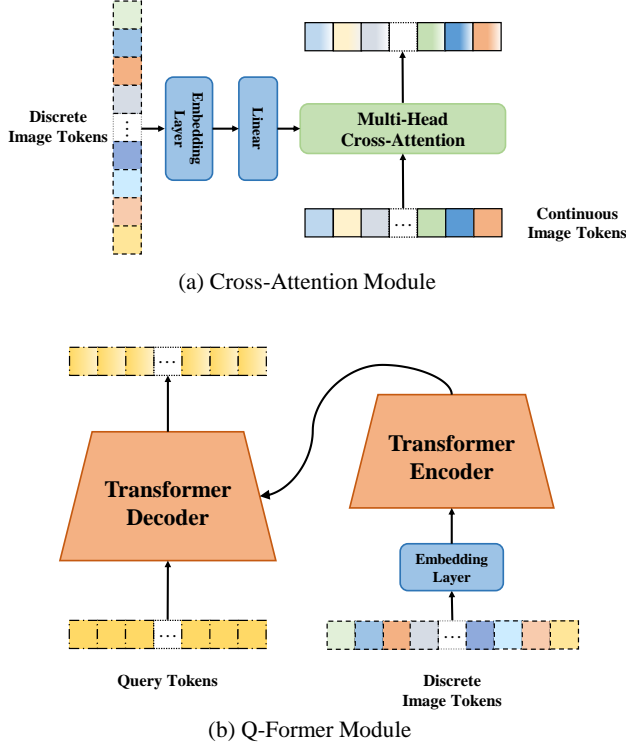


Figure 2. Fusion Module.

4.2. From Discrete to Continuous Tokens

In the second stage, the goal is to train the main body of our framework, a hybrid autoregressive model that generates the fine-grained image features, continuous-valued tokens, conditioned on the above discrete-valued tokens, as illustrated in Figure.1. We adopt the Masked Autoencoder (MAE) (He et al., 2022) with bidirectional attention as our hybrid autoregressive model. In training of this stage, we use the above discrete-valued model to generate the next discrete-valued token conditioned on the class token and ground true tokens before this position that are produced by the discrete image tokenizer. For better interacting between discrete-valued and continuous-valued tokens, we insert a fusion module into the MAE. Specifically, we employ the continuous image tokenizer (Kingma, 2013) to encode the input image $x \in \mathbb{R}^{H \times W \times 3}$ as continuous-valued tokens $z \in \mathbb{R}^{h \times w \times d}$. The downsampling rate is same as the discrete image tokenizer. Then we randomly sample a masking rate m_r from a truncated Gaussian distribution following Li et al. (2023b). Uniformly, we convert the 2-dimensional continuous-valued image tokens into a 1-dimensional sequence $z_c = [z_{c,1}, \dots, z_{c,i}, \dots, z_{c,h \cdot w}]$ and then mask out $m_r \cdot h \cdot w$ tokens which is replaced with a learnable mask token $[M]$. Besides, 64 identical class tokens are padded as the prefix of the input sequence for improving the stability

and capacity of encoding (Li et al., 2024a). In the encoder of MAE, the encoding process is to primarily aggregate available and reliable information. In the decoder of MAE, the $[M]$ tokens gradually acquire the important information to generate the indispensable condition z . Afterwards, we utilize a lightweight MLP to iteratively denoise conditioned on z and timestep t , while the training objective is to calculate matching scores utilizing mean-squared error, as shown in the Eq.2. For executing autoregressive generation, we introduce random orders (Li et al., 2024a), where the input continuous-valued token sequence is shuffled at random. In training, we mask out the last $m_r \cdot h \cdot w$ tokens in the shuffled sequence. And we predict token of next position in the generated random order in inference.

4.3. Fusion Modules

For connecting the two stages to achieve progressive generating, we propose two types of fusion module: cross-attention module and q-former module.

Cross-Attention Module. Our cross-attention module is shown in the Figure.2 (a), which is preceded by a normalization layer. In the MAE (He et al., 2022), the original block in encoder and decoder only contain self-attention and feedforward module. When the cross-attention module is selected as the fusion module, we add our cross-attention module between self-attention and feedforward module to carry out interaction. The cross-attention module is formulated as follows:

$$h_q = \text{Linear}_\theta(\text{Embed}_\theta(q)) \quad (4)$$

$$Q = W_q h_c, K = W_k h_q, V = W_v h_q \quad (5)$$

$$\text{CrossAttention}(Q, K, V) = \text{Softmax}\left(\frac{QK^T}{\sqrt{d}}\right)V \quad (6)$$

where $h_c \in \mathbb{R}^{hw \times d}$ and $h_q \in \mathbb{R}^{hw \times d}$ severally denote the hidden states of continuous-valued tokens and discrete-valued tokens. $W_q \in \mathbb{R}^{d \times d}$, $W_k \in \mathbb{R}^{d \times d}$, $W_v \in \mathbb{R}^{d \times d}$ are the learnable projection matrices, respectively.

Q-Former Module. As shown in Figure.2 (b), the q-former module is a encoder-decoder architecture based on Transformer (Vaswani, 2017). The input of q-former module include the features of discrete tokens $h_q \in \mathbb{R}^{hw \times d}$ and L learnable query embeddings $e_{query} \in \mathbb{R}^{L \times d_{query}}$, where L is the number of query embeddings and d_{query} is the dim of query embedding. The query embeddings are introduced to refine coarse-grained image features from the sequences of hw discrete-valued tokens generated in the first stage. This is similar with the queries introduced in BLIP-2 (Li et al., 2023a), GILL (Koh et al., 2024) and Minigpt-5 (Zheng et al., 2023) for extracting image features. Afterward, the output features $h_q \in \mathbb{R}^{L \times d}$ are concatenated with the class to-

Table 1. The performance of our model on ImageNet 256×256 benchmark. "Token" refers to token type used by the generation model where "discrete" and "continuous" denote the token generated by discrete tokenizer (eg. VQGAN) and continuous tokenizer (eg. VAE), respectively. "both" contains the above two type of tokens. "Type" is the type of generation model including diffusion model (Diff.), masked model (Mask.), autoregressive model (AR) and visual autoregressive model (VAR). "#Step" is the number of inference step. In this table, the parameters of our model contain discrete-valued generation model (111M) and continuous-valued generation model.

Token	Type	Model	#Params	#Steps	with CFG				without CFG			
					FID↓	IS↑	Pre.↑	Rec.↑	FID↓	IS↑	Pre.↑	Rec.↑
discrete	Diff.	LDM-8 (Rombach et al., 2022)	258M	200	7.76	209.5	0.74	0.35	15.51	79.0	0.65	0.63
	Mask.	MaskGIT (Chang et al., 2022)	227M	8	6.18	1.821	0.80	0.51	-	-	-	-
	AR	VQGAN (Esser et al., 2021)	227M	256	18.65	80.4	0.78	0.26	-	-	-	-
		LlamaGen-B (Sun et al., 2024)	111M	256	5.46	193.6	0.84	0.46	26.26	48.1	0.59	0.62
		LlamaGen-XL (Sun et al., 2024)	775M	256	3.39	227.1	0.81	0.54	19.42	66.2	0.61	0.67
continuous	Diff.	LDM-4 (Rombach et al., 2022)	400M	250	3.60	247.7	0.87	0.48	10.56	103.5	0.71	0.62
		DiT-XL/2 (Peebles & Xie, 2023)	675M	250	2.27	278.2	0.83	0.57	9.62	121.5	0.67	0.67
	AR	GIVT (Tschannen et al., 2023)	304M	256	3.35	-	0.84	0.53	5.67	-	0.75	0.59
		MAR-B (Li et al., 2024a)	208M	256	2.31	281.7	0.82	0.57	3.48	192.4	0.78	0.58
		MAR-L (Li et al., 2024a)	479M	256	1.78	296.0	0.81	0.60	2.60	221.4	0.79	0.60
	VAR	HART-d20 (Tang et al., 2024)	649M	10	2.39	316.4	-	-	-	-	-	-
both	AR	D2C-B with Cross-Attention Module	389M	64	2.25	266.8	0.77	0.63	3.58	227.9	0.82	0.52
		D2C-B with Q-Former Module	362M	64	2.09	265.2	0.77	0.63	3.39	234.3	0.83	0.53
				256	2.06	266.7	0.77	0.62	3.35	235.0	0.83	0.53
		D2C-L with Q-Former Module	633M	64	1.73	285.7	0.77	0.64	3.14	264.5	0.84	0.53
				192	1.71	285.1	0.78	0.64	3.20	269.3	0.85	0.53

kens and continuous-valued tokens. In the subsequent MAE model, the discrete-valued and continuous-valued tokens engage in self-attention interaction.

$$h_{query} = QFormer_{\theta}(e_{query}, Embed_{\theta}(q)) \quad (7)$$

4.4. Discussions

In the HART model (Tang et al., 2024), the discrete-valued and continuous-valued tokens are generated by only a re-designed hybrid image tokenizer. The MLP in HART is employed for iteratively denoising to predict the residual tokens that offsets the information loss because of vector quantization. The performance of a continuous-valued generative model is its upper limit. Besides, in the Disco-Diff model (Xu et al., 2024), a few complementary discrete-valued tokens are inferred through an encoder in training. The complementary discrete-valued tokens capture the global appearance patterns, such as style and color, but do not represent a specific and entire image. The motivation of Disco-Diff is to simplify the learning process of continuous-valued diffusion models. In our method, the discrete-valued and continuous-valued tokens are introduced by discrete and continuous image tokenizers, respectively. And we design a unique two-stage framework to realize progressive image generation. Although our diffusion MLP is same as MAR (Li et al., 2024a), we fuse the two types of tokens with the fusion module to learn a more strong denoising condition.

5. Experiments

5.1. Implementation Details

Image Tokenizer. We use the VQGAN (Esser et al., 2021) model from LlamaGen (Sun et al., 2024) as our discrete image tokenizer, which tokenizes a 256×256 image into 256 discrete-valued tokens with a 16384 codebook size. And the VAE model (Rombach et al., 2022) from LDM (Rombach et al., 2022) is employed as our continuous image tokenizer with a downsampling factor 16.

Dataset. Our models are trained on ImageNet (Deng et al., 2009) which contains 1000 object classes of images, a total of 1, 281, 167 training images. To reduce training cost, we pretokenize each image from training set into discrete-valued tokens and continuous-valued tokens with VQGAN and VAE, respectively. Before this, each image is preprocessed with center cropping and horizontal flipping augmentation.

Classifier-free Guidance. The classifier-free guidance (Ho & Salimans, 2022) method has been demonstrated to effectively improve the generative image quality in conditional image generation tasks. During the training phase, we drop out both the class tokens and discrete-valued tokens with a probability 0.1 that are replaced with the learnable and fake class token and discrete-valued tokens, respectively. And in inference, the predicted noise follows the equation: $\varepsilon =$

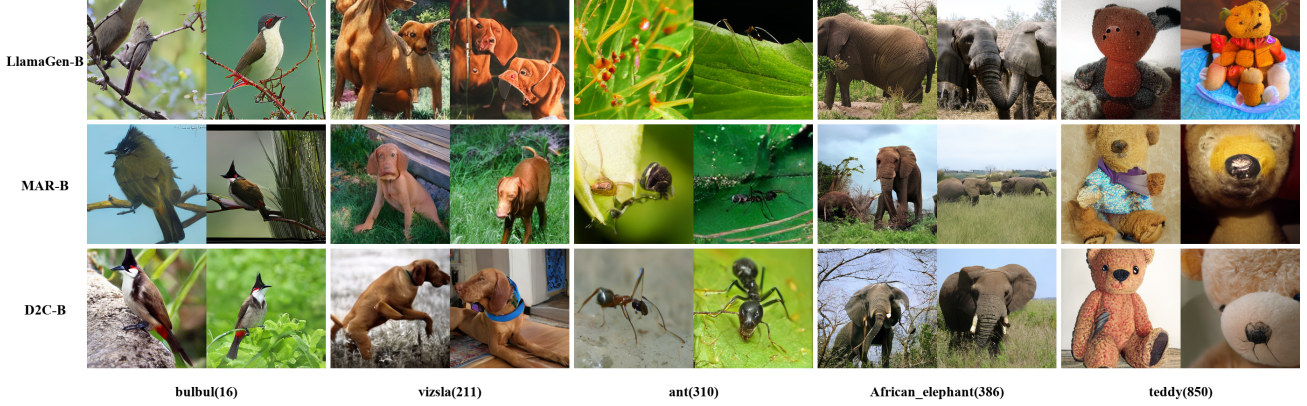


Figure 3. Visualization of samples across various classes and models.

$\varepsilon_{\theta}(x_t|t, z_{uncond}) + \omega \cdot (\varepsilon_{\theta}(x_t|t, z_{cond}) - \varepsilon_{\theta}(x_t|t, z_{uncond}))$, where ω is the guidance scale, and t is the timestep, z_{cond} is the discrete and continuous-valued tokens condition and z_{uncond} is the fake tokens.

Training. For convenience, we initialize our discrete-valued autoregressive model using the pretrained LlamaGen-B model (Sun et al., 2024) and then freeze all parameters. Our hybrid autoregressive models of the second stage, D2C-B and D2C-L are trained for 800 epochs using the AdamW optimizer with $\beta_1 = 0.9$, $\beta_2 = 0.95$ and weight decay as 0.02. The base learning rate is set $5e-5$ per 256 batch size and the learning rate is linearly increased with the training step at first 100 epochs, then it remains constant. Moreover, we maintain the exponential moving average (EMA) of the model parameters with a momentum of 0.9999. In training, we randomly sample a mask rate from a truncated Gaussian distribution [0.7, 1.0]. The discrete token embedding layer of hybrid autoregressive model is initialized by the discrete-valued autoregressive model and freed.

Inference and Evaluation. We generate each image with a simpler linear guidance schedule and progressively reduce the masking ratio from 1.0 to 0 with a cosine schedule. The discrete-valued autoregressive model produces the discrete-valued tokens with multinomial sampling strategy only given the class. In addition, we use Fréchet Inception Distance (FID) (Heusel et al., 2017) as the primary evaluation metric, while Inception Score (IS) (Salimans et al., 2016), as auxiliary evaluation metric.

5.2. Main Results

In Table.1, we compare our model with popular image generation models, include discrete-valued models (Esser et al., 2021; Rombach et al., 2022; Chang et al., 2022; Yu et al., 2023; 2024b; Weber et al., 2024; Sun et al., 2024; Yu et al.,

2024a), continuous-valued models (Rombach et al., 2022; Peebles & Xie, 2023; Tschannen et al., 2023; Li et al., 2024a) and both-based models (Tang et al., 2024). Compared with them, our models achieve superior performance with classifier-free guidance. Specifically, D2C-B with Q-Former Module achieves an FID score 2.09 only using 64 steps, significantly outperforming the LlamaGen-B (Sun et al., 2024) and MAR-B (Li et al., 2024a) models. And it achieves $3.5\times$ higher speed than MAR in inference. When using 256 steps, D2C-B with Q-Former Module further improve the FID score to 2.06. In addition, we also get better results than the HART model of the same type (Tang et al., 2024). Besides, we also explore the bigger model size, D2C-L with Q-Former Module getting an FID score 1.71, where the consistent performance improvement is observed when scaling up model size. These results confirm that hybrid condition merging discrete and continuous token contains more abundant information compared with the loss-less continuous-valued tokens. On the other hand, we notice that the performance of our models without classifier-free guidance is not satisfactory. Because the discrete-valued tokens are sampled with classifier-free guidance when not using classifier-free guidance to generate continuous-valued tokens. This reduces diversity of generated image but significantly improves the IS score.

Q-Former vs Cross-Attention. We conduct experiments with diffusion fusion modules: cross-attention module and q-former module. Obviously, our model with q-former module gets better results compared with cross-attention module. This indicates that the query tokens in the q-former module are able to refine efficient information and discard useless information from discrete image features.

Visualization. As shown in Figure.3, we visualize generated samples by our model, MAR (Li et al., 2024a) and LlamaGen (Sun et al., 2024), which demonstrates that our

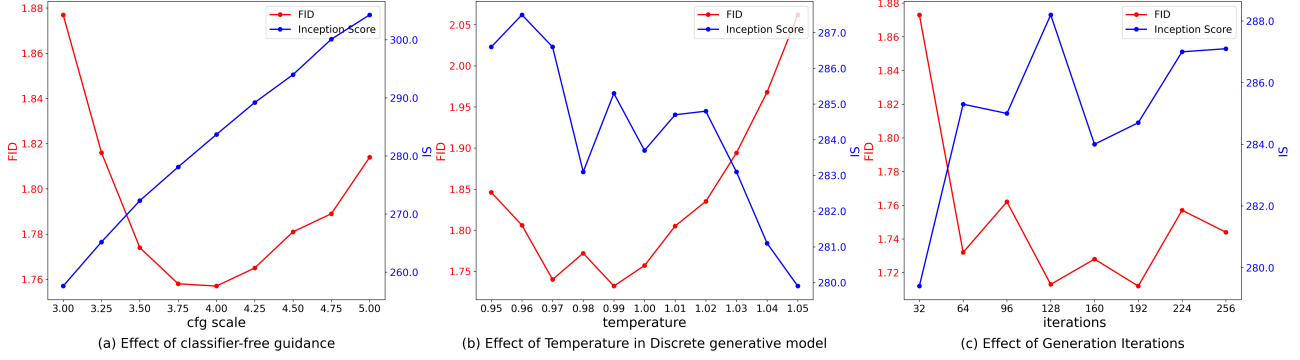


Figure 4. The variation of FID and IS with respect to different hyper-parameter: cfg scale, temperature of discrete-valued generative model and number of generation iterations.

Table 2. Comparison of different query tokens in q-former refiner on class-conditional Generation on ImageNet 256×256 benchmark, where each model with 3 MLP is trained to 400 epochs.

Number of query tokens	with CFG		without CFG	
	FID↓	IS↑	FID↓	IS↑
16	2.43	263.8	3.70	227.7
32	2.41	258.8	3.71	228.0
64	11.70	81.1	7.34	115.1

model is capable of generating high-quality and diverse images.

5.3. Ablation Studies

Number of Query Tokens and Q-former Architecture.

As shown in Table.2, we conduct ablation experiments on assess the impact about number of query tokens on model performance. In the MAR model (Li et al., 2024a), 64 identical class tokens are padded at the start of the encoder sequence. In our model, a part of class tokens are replaced with query tokens extracting feature from discrete-valued tokens. Specifically, we examine the effect of 16, 32 and 64 query tokens, respectively. In order to balance efficiency and performance, we chose 16 query tokens in the q-former module. Besides, we compare different q-former architecture in Table.3. It is obvious that the q-former with encoder-decoder architecture gets optimal performance. It also shows that aggregating reliable information is indispensable before extracting the important information from the discrete-valued tokens.

Effect of Classifier-free Guidance and Temperature of Generating Discrete Token. In Figure.4 (a), we conduct ablation experiments on different classifier-free guidance scale.

Table 3. Comparison of different architecture of q-former refiner on class-conditional Generation on ImageNet 256×256 benchmark, where each model with 3 MLP is trained to 400 epochs and the number of query tokens is 16.

Q-former Architecture	with CFG		without CFG	
	FID↓	IS↑	FID↓	IS↑
Decoder	2.55	270.3	3.81	223.1
Encoder-Decoder	2.43	263.8	3.70	227.7

Increasing the classifier-free guidance scale can improve the quality of generated images but reduce the variety, which balances the diversity and fidelity of images. On the other hand, the temperature in sampling the discrete token has a similar effect with classifier-free guidance scale in Figure.4 (b). In our model with q-former module, the optimal performance is achieved while the classifier-free guidance scale is set to 4.0. And temperature of discrete-valued generation model to 0.99 is the best choice with classifier-free guidance.

Effect of Generation Iterations. Figure.4 (c) show FID and IS metrics variations with the number of generation Iterations. With the increase of the number of generation Iterations, both FID and IS metrics show a trend of increasing first, then slight fluctuation. Our model achieves the best result at 192 generation Iterations. In fact, using 64 steps in inference is sufficient to achieve a strong generation quality.

6. Conclusion

In this paper, we propose D2C, a two-stage hybrid autoregressive model, which merges the discrete-valued tokens from a small discrete-valued image generation model with the continuous-valued tokens for enhancing image synthesis

in the class-to-image task. In order to connect both, we design two kinds of fusion modules, cross-attention module and q-former module, to achieve fine-grained continuous-valued tokens generation based on coarse-grained discrete-valued tokens. Our experiment results indicate that our model surpasses both discrete-valued and continuous-valued model in generation image quality. Moreover, the effectiveness of fusing discrete and continuous-valued tokens in autoregressive models is proved. We hope that this work contributes to advancing hybrid model combining continuous-valued and discrete-valued for image generation.

Impact Statement

This paper presents work whose goal is to improve the image generation quality through fusing discrete and continuous-valued tokens in the class-to-image task. There are many potential societal consequences of our work, none which we feel must be specifically highlighted here.

References

- Bai, Z., Gao, J., Gao, Z., Wang, P., Zhang, Z., He, T., and Shou, M. Z. Factorized visual tokenization and generation. *arXiv preprint arXiv:2411.16681*, 2024.
- Bao, F., Nie, S., Xue, K., Cao, Y., Li, C., Su, H., and Zhu, J. All are worth words: A vit backbone for diffusion models. In *Proceedings of the IEEE/CVF conference on computer vision and pattern recognition*, pp. 22669–22679, 2023.
- Betker, J., Goh, G., Jing, L., Brooks, T., Wang, J., Li, L., Ouyang, L., Zhuang, J., Lee, J., Guo, Y., et al. Improving image generation with better captions. *Computer Science*. <https://cdn.openai.com/papers/dall-e-3.pdf>, 2(3): 8, 2023.
- Cao, S., Yin, Y., Huang, L., Liu, Y., Zhao, X., Zhao, D., and Huang, K. Efficient-vqgan: Towards high-resolution image generation with efficient vision transformers. In *Proceedings of the IEEE/CVF International Conference on Computer Vision*, pp. 7368–7377, 2023.
- Chang, H., Zhang, H., Jiang, L., Liu, C., and Freeman, W. T. Maskgit: Masked generative image transformer. In *Proceedings of the IEEE/CVF Conference on Computer Vision and Pattern Recognition*, pp. 11315–11325, 2022.
- Chang, H., Zhang, H., Barber, J., Maschinot, A., Lezama, J., Jiang, L., Yang, M.-H., Murphy, K., Freeman, W. T., Rubinstein, M., et al. Muse: Text-to-image generation via masked generative transformers. *arXiv preprint arXiv:2301.00704*, 2023.
- Chen, J., Yu, J., Ge, C., Yao, L., Xie, E., Wu, Y., Wang, Z., Kwok, J., Luo, P., Lu, H., et al. Pixart- α : Fast training of diffusion transformer for photorealistic text-to-image synthesis. *arXiv preprint arXiv:2310.00426*, 2023.
- Chen, M., Radford, A., Child, R., Wu, J., Jun, H., Luan, D., and Sutskever, I. Generative pretraining from pixels. In *International conference on machine learning*, pp. 1691–1703. PMLR, 2020.
- Chen, W., Niu, L., Lu, Z., Meng, F., and Zhou, J. Maskmamba: A hybrid mamba-transformer model for masked image generation. *arXiv preprint arXiv:2409.19937*, 2024.
- Deng, J., Dong, W., Socher, R., Li, L.-J., Li, K., and Fei-Fei, L. Imagenet: A large-scale hierarchical image database. In *2009 IEEE conference on computer vision and pattern recognition*, pp. 248–255. Ieee, 2009.
- Esser, P., Rombach, R., and Ommer, B. Taming transformers for high-resolution image synthesis. In *Proceedings of the IEEE/CVF conference on computer vision and pattern recognition*, pp. 12873–12883, 2021.
- Fan, L., Li, T., Qin, S., Li, Y., Sun, C., Rubinstein, M., Sun, D., He, K., and Tian, Y. Fluid: Scaling autoregressive text-to-image generative models with continuous tokens. *arXiv preprint arXiv:2410.13863*, 2024.
- Gu, J., Wang, Y., Zhang, Y., Zhang, Q., Zhang, D., Jaitly, N., Susskind, J., and Zhai, S. Dart: Denoising autoregressive transformer for scalable text-to-image generation. *arXiv preprint arXiv:2410.08159*, 2024.
- He, K., Chen, X., Xie, S., Li, Y., Dollár, P., and Girshick, R. Masked autoencoders are scalable vision learners. In *Proceedings of the IEEE/CVF conference on computer vision and pattern recognition*, pp. 16000–16009, 2022.
- Heusel, M., Ramsauer, H., Unterthiner, T., Nessler, B., and Hochreiter, S. Gans trained by a two time-scale update rule converge to a local nash equilibrium. *Advances in neural information processing systems*, 30, 2017.
- Ho, J. and Salimans, T. Classifier-free diffusion guidance. *arXiv preprint arXiv:2207.12598*, 2022.
- Ho, J., Jain, A., and Abbeel, P. Denoising diffusion probabilistic models. *Advances in neural information processing systems*, 33:6840–6851, 2020.
- Ho, J., Chan, W., Saharia, C., Whang, J., Gao, R., Gritsenko, A., Kingma, D. P., Poole, B., Norouzi, M., Fleet, D. J., et al. Imagen video: High definition video generation with diffusion models. *arXiv preprint arXiv:2210.02303*, 2022.
- Huang, M., Mao, Z., Chen, Z., and Zhang, Y. Towards accurate image coding: Improved autoregressive image

- generation with dynamic vector quantization. In *Proceedings of the IEEE/CVF Conference on Computer Vision and Pattern Recognition*, pp. 22596–22605, 2023a.
- Huang, M., Mao, Z., Wang, Q., and Zhang, Y. Not all image regions matter: Masked vector quantization for autoregressive image generation. In *Proceedings of the IEEE/CVF Conference on Computer Vision and Pattern Recognition*, pp. 2002–2011, 2023b.
- Kingma, D. P. Auto-encoding variational bayes. *arXiv preprint arXiv:1312.6114*, 2013.
- Koh, J. Y., Fried, D., and Salakhutdinov, R. R. Generating images with multimodal language models. *Advances in Neural Information Processing Systems*, 36, 2024.
- Lee, D., Kim, C., Kim, S., Cho, M., and Han, W.-S. Autoregressive image generation using residual quantization. In *Proceedings of the IEEE/CVF Conference on Computer Vision and Pattern Recognition*, pp. 11523–11532, 2022.
- Li, J., Li, D., Savarese, S., and Hoi, S. Blip-2: Bootstrapping language-image pre-training with frozen image encoders and large language models. In *International conference on machine learning*, pp. 19730–19742. PMLR, 2023a.
- Li, T., Chang, H., Mishra, S., Zhang, H., Katabi, D., and Krishnan, D. Mage: Masked generative encoder to unify representation learning and image synthesis. In *Proceedings of the IEEE/CVF Conference on Computer Vision and Pattern Recognition*, pp. 2142–2152, 2023b.
- Li, T., Tian, Y., Li, H., Deng, M., and He, K. Autoregressive image generation without vector quantization. *arXiv preprint arXiv:2406.11838*, 2024a.
- Li, X., Qiu, K., Chen, H., Kuen, J., Gu, J., Raj, B., and Lin, Z. Imagefolder: Autoregressive image generation with folded tokens. *arXiv preprint arXiv:2410.01756*, 2024b.
- Liu, D., Zhao, S., Zhuo, L., Lin, W., Qiao, Y., Li, H., and Gao, P. Lumina-mgpt: Illuminate flexible photorealistic text-to-image generation with multimodal generative pretraining. *arXiv preprint arXiv:2408.02657*, 2024.
- Luo, Z., Shi, F., Ge, Y., Yang, Y., Wang, L., and Shan, Y. Open-magvit2: An open-source project toward democratizing auto-regressive visual generation. *arXiv preprint arXiv:2409.04410*, 2024.
- Ma, X., Zhou, M., Liang, T., Bai, Y., Zhao, T., Chen, H., and Jin, Y. Star: Scale-wise text-to-image generation via auto-regressive representations. *arXiv preprint arXiv:2406.10797*, 2024.
- Pang, Z., Zhang, T., Luan, F., Man, Y., Tan, H., Zhang, K., Freeman, W. T., and Wang, Y.-X. Randar: Decoder-only autoregressive visual generation in random orders. *arXiv preprint arXiv:2412.01827*, 2024.
- Peebles, W. and Xie, S. Scalable diffusion models with transformers. In *Proceedings of the IEEE/CVF International Conference on Computer Vision*, pp. 4195–4205, 2023.
- Podell, D., English, Z., Lacey, K., Blattmann, A., Dockhorn, T., Müller, J., Penna, J., and Rombach, R. Sdxl: Improving latent diffusion models for high-resolution image synthesis. *arXiv preprint arXiv:2307.01952*, 2023.
- Razavi, A., Van den Oord, A., and Vinyals, O. Generating diverse high-fidelity images with vq-vae-2. *Advances in neural information processing systems*, 32, 2019.
- Rombach, R., Blattmann, A., Lorenz, D., Esser, P., and Ommer, B. High-resolution image synthesis with latent diffusion models. In *Proceedings of the IEEE/CVF conference on computer vision and pattern recognition*, pp. 10684–10695, 2022.
- Salimans, T., Goodfellow, I., Zaremba, W., Cheung, V., Radford, A., and Chen, X. Improved techniques for training gans. *Advances in neural information processing systems*, 29, 2016.
- Shazeer, N. Glu variants improve transformer. *arXiv preprint arXiv:2002.05202*, 2020.
- Shi, F., Luo, Z., Ge, Y., Yang, Y., Shan, Y., and Wang, L. Taming scalable visual tokenizer for autoregressive image generation. *arXiv preprint arXiv:2412.02692*, 2024.
- Song, J., Meng, C., and Ermon, S. Denoising diffusion implicit models. *arXiv preprint arXiv:2010.02502*, 2020.
- Su, J., Ahmed, M., Lu, Y., Pan, S., Bo, W., and Liu, Y. Roformer: Enhanced transformer with rotary position embedding. *Neurocomputing*, 568:127063, 2024.
- Sun, P., Jiang, Y., Chen, S., Zhang, S., Peng, B., Luo, P., and Yuan, Z. Autoregressive model beats diffusion: Llama for scalable image generation. *arXiv preprint arXiv:2406.06525*, 2024.
- Tang, H., Wu, Y., Yang, S., Xie, E., Chen, J., Chen, J., Zhang, Z., Cai, H., Lu, Y., and Han, S. Hart: Efficient visual generation with hybrid autoregressive transformer. *arXiv preprint arXiv:2410.10812*, 2024.
- Touvron, H., Lavril, T., Izacard, G., Martinet, X., Lachaux, M.-A., Lacroix, T., Rozière, B., Goyal, N., Hambro, E., Azhar, F., et al. Llama: Open and efficient foundation language models. *arXiv preprint arXiv:2302.13971*, 2023.

- Tschannen, M., Eastwood, C., and Mentzer, F. Givit: Generative infinite-vocabulary transformers. *arXiv e-prints*, pp. arXiv-2312, 2023.
- Van Den Oord, A., Kalchbrenner, N., and Kavukcuoglu, K. Pixel recurrent neural networks. In *International conference on machine learning*, pp. 1747–1756. PMLR, 2016.
- Van Den Oord, A., Vinyals, O., et al. Neural discrete representation learning. *Advances in neural information processing systems*, 30, 2017.
- Vaswani, A. Attention is all you need. *Advances in Neural Information Processing Systems*, 2017.
- Weber, M., Yu, L., Yu, Q., Deng, X., Shen, X., Cremers, D., and Chen, L.-C. Maskbit: Embedding-free image generation via bit tokens. *arXiv preprint arXiv:2409.16211*, 2024.
- Wu, Y., Zhang, Z., Chen, J., Tang, H., Li, D., Fang, Y., Zhu, L., Xie, E., Yin, H., Yi, L., et al. Vila-u: a unified foundation model integrating visual understanding and generation. *arXiv preprint arXiv:2409.04429*, 2024.
- Xie, J., Mao, W., Bai, Z., Zhang, D. J., Wang, W., Lin, K. Q., Gu, Y., Chen, Z., Yang, Z., and Shou, M. Z. Show-o: One single transformer to unify multimodal understanding and generation. *arXiv preprint arXiv:2408.12528*, 2024.
- Xu, Y., Corso, G., Jaakkola, T., Vahdat, A., and Kreis, K. Disco-diff: Enhancing continuous diffusion models with discrete latents. *arXiv preprint arXiv:2407.03300*, 2024.
- Yu, J., Li, X., Koh, J. Y., Zhang, H., Pang, R., Qin, J., Ku, A., Xu, Y., Baldridge, J., and Wu, Y. Vector-quantized image modeling with improved vqgan. *arXiv preprint arXiv:2110.04627*, 2021.
- Yu, J., Xu, Y., Koh, J. Y., Luong, T., Baid, G., Wang, Z., Vasudevan, V., Ku, A., Yang, Y., Ayan, B. K., et al. Scaling autoregressive models for content-rich text-to-image generation. *arXiv preprint arXiv:2206.10789*, 2(3):5, 2022.
- Yu, L., Lezama, J., Gundavarapu, N. B., Versari, L., Sohn, K., Minnen, D., Cheng, Y., Birodkar, V., Gupta, A., Gu, X., et al. Language model beats diffusion-tokenizer is key to visual generation. *arXiv preprint arXiv:2310.05737*, 2023.
- Yu, Q., He, J., Deng, X., Shen, X., and Chen, L.-C. Randomized autoregressive visual generation. *arXiv preprint arXiv:2411.00776*, 2024a.
- Yu, Q., Weber, M., Deng, X., Shen, X., Cremers, D., and Chen, L.-C. An image is worth 32 tokens for reconstruction and generation. *arXiv preprint arXiv:2406.07550*, 2024b.
- Zhang, B. and Sennrich, R. Root mean square layer normalization. *Advances in Neural Information Processing Systems*, 32, 2019.
- Zhang, B., Wang, H., Luo, C., Li, X., Liang, G., Ye, Y., Qi, X., and He, Y. Codebook transfer with part-of-speech for vector-quantized image modeling. In *Proceedings of the IEEE/CVF Conference on Computer Vision and Pattern Recognition*, pp. 7757–7766, 2024a.
- Zhang, J., Zhan, F., Theobalt, C., and Lu, S. Regularized vector quantization for tokenized image synthesis. In *Proceedings of the IEEE/CVF Conference on Computer Vision and Pattern Recognition*, pp. 18467–18476, 2023.
- Zhang, Q., Dai, X., Yang, N., An, X., Feng, Z., and Ren, X. Var-clip: Text-to-image generator with visual autoregressive modeling. *arXiv preprint arXiv:2408.01181*, 2024b.
- Zhao, C., Song, Y., Wang, W., Feng, H., Ding, E., Sun, Y., Xiao, X., and Wang, J. Monoformer: One transformer for both diffusion and autoregression. *arXiv preprint arXiv:2409.16280*, 2024.
- Zheng, C. and Vedaldi, A. Online clustered codebook. In *Proceedings of the IEEE/CVF International Conference on Computer Vision*, pp. 22798–22807, 2023.
- Zheng, C., Vuong, T.-L., Cai, J., and Phung, D. Movq: Modulating quantized vectors for high-fidelity image generation. *Advances in Neural Information Processing Systems*, 35:23412–23425, 2022.
- Zheng, K., He, X., and Wang, X. E. Minigpt-5: Interleaved vision-and-language generation via generative tokens. *arXiv preprint arXiv:2310.02239*, 2023.
- Zhou, C., Yu, L., Babu, A., Tirumala, K., Yasunaga, M., Shamis, L., Kahn, J., Ma, X., Zettlemoyer, L., and Levy, O. Transfusion: Predict the next token and diffuse images with one multi-modal model. *arXiv preprint arXiv:2408.11039*, 2024.